Comonomer Compositional Distribution and Thermal and Morphological Characteristics of Bacterial Poly(3-hydroxybutyrate- c o -3-hydroxyvalerate)s with High 3-Hydroxyvalerate Content

ARTICLE *in* BIOMACROMOLECULES · FEBRUARY 2001

Impact Factor: 5.75 · DOI: 10.1021/bm010128o · Source: PubMed

Comonomer Compositional Distribution and Thermal and Morphological Characteristics of Bacterial Poly(3-hydroxybutyrate-*co*-3-hydroxyvalerate)s with High 3-Hydroxyvalerate Content

Yi Wang,[†] Shino Yamada,[†] Naoki Asakawa,[†] Tsuneo Yamane,[‡] Naoko Yoshie,[†] and Yoshio Inoue*,[†]

Department of Biomolecular Engineering, Tokyo Institute of Technology, 4259 Nagatsuta, Midori-ku, Yokohama 226-8501, Japan; and Department of Biological Mechanisms and Functions, Graduate School of Bio- and Agro-Sciences, Nagoya University, Chikusa-ku, Nagoya 464-8601, Japan

Received August 9, 2001

The comonomer compositional distribution and thermal and morphological characteristics were investigated for five bacterially synthesized poly(3-hydroxybutyrate-*co*-3-hydroxyvalerate) [P(3HB-*co*-3HV)] samples with 3HV content of 45, 49, 70, 80, and 96 mol %. All these samples were fractionated into many fractions with widely different 3HV content by changing solvent/nonsolvent volume ratio of chloroform/*n*-heptane mixtures. Bacterial P(3HB-*co*-3HV) samples investigated in this study were found to have broad comonomer compositional distribution. The tendencies of the fractional precipitation of the P((3HB-*co*-3HV)s with 3HV content lower than 60 mol % and those with 3HV higher than 80 mol % were found to be contrary. The 3HV content dependences of the thermal properties and crystalline structures were investigated for bacterial poly(3-hydroxybutyrate) [P(3HB)] and a series of compositionally well-fractionated P(3HB-*co*-3HV) samples with 3HV content ranged from 14 to 98 mol % by DSC, WAXD, and solid-state ^{13}C NMR. It was found that P(3HB-*co*-3HV) samples with 3HV content lower than about 47 mol % form the crystalline lattice having the P(3HB) homopolymer type lattice including the 3HV unit as the crystal constituent, and those with a 3HV content higher than about 52 mol % form the crystalline lattice having the P(3HV) homopolymer type lattice including the 3HB units. Thus, P(3HB-*co*-3HV)s show the crystalline structural change in a very narrow range of 3HV content.

Introduction

Bacterial polyhydroxyalkanoates (PHAs) are natural biodegradable thermoplastics produced as intracellular energy and carbon storage materials by various microorganisms.[1,2] A series of PHA copolyesters, such as poly(3-hydroxybutyrate-*co*-3-hydroxyvalerate) [P(3HB-*co*-3HV)], poly(3-hydroxybutyrate-*co*-3-hydroxypropionate) [P(3HB-*co*-3HP)], and poly(3-hydroxybutyrate-*co*-4-hydroxybutyrate) [P(3HB-*co*-4HB)], have been biosynthesized.[1,2] The sequence distributions of the bacterial copolymers have been found to be random.[3] In general, morphology and several physical properties of copolymers strongly depend on their comonomer composition as well as their sequence structure.[4] Kamiya et al. have indicated the complex comonomer compositions of the bacterially synthesized P(3HB-*co*-3HV)s by statistical analyses of the sequence structures.[5] For the bacterial copolyester P(3HB-*co*-3HV)s with composition of around 41 mol % 3HV produced by *Ralstonia eutropha*, the coexistence of both poly(3-hydroxybutyrate) [P(3HB)] and poly(3-hydroxyvalerate) [P(3HV)] homopolymer type crystal phases has been found by solid-state ^{13}C NMR.[6] To clarify the origin of these findings, Mitomo et al. have attempted to fractionate the bacterial P(3HB-*co*-3HV)s via the acetone/water mixed solvent.[7] Their results demonstrated that bacterial P(3HB-*co*-3HV)s have broad comonomer compositional distribution. On the other hand, the microstructure of the commercially available bacterial P(3HB-*co*-3HV) samples with the 3HV contents less than 25 mol % have been also investigated by Yoshie et al. via a chloroform/*n*-heptane fractionating procedure.[8] The copolymers could be fractionated into fractions with the 3HV contents ranged from about 5 to 40 mol %. As the side chain of the 3HV unit is the ethyl group instead of the methyl group of the 3HB unit, the polarity of the P(3HB-*co*-3HV) chain depends on the monomer composition. Therefore, when *n*-heptane is added into the solution in chloroform, a series of P(3HB-*co*-3HV) fractions are gradually precipitated in the order of increasing 3HV content. However, the 3HV contents of previously reported original unfractionated P(3HB-*co*-3HV) samples were less than 25 mol %, and those of the fractions were less than 40 mol %.

It has not been studied whether the copolymer P(3HB-*co*-3HV)s with higher 3HV content have broad comonomer compositional distribution and can be fractionated in the same way as that found for P(3HB-*co*-3HV) with low 3HV content. The compositional fractionation by acetone/water

* To whom correspondence should be addressed. E-mail: yinoue@bio.titech.ac.jp.
[†] Tokyo Institute of Technology.
[‡] Nagoya University.

10.1021/bm010128o CCC: $20.00
Published on Web 10/06/2001

or chloroform/*n*-heptane systems was considered to be caused mainly by the difference in comonomer composition and sometimes the molecular weight. However, it has never been discussed whether other factors, e.g., crystallizability would influence the fractionation. As it has been known, polymers can be fractionated by precipitation from a solvent/nonsolvent mixture carried out by adding the nonsolvent to a dilute solution of the polymer. But it is essential that the polymer-rich phase be amorphous rather than crystalline and that other parameters influencing the separation, be controlled.[9] However, the crystallizability of P(3HB-*co*-3HV)s was different with 3HV content. It decreased with 3HV content from 0 [P(3HB)] to 40−50 mol %, then increased.[8] Furthermore, the spherulite growth rates of the copolymers were great.[8] Thus, it is very possible that the crystallizability would influence the fractionation of the copolymer.

On the other hand, it is well-known that P(3HB-*co*-3HV) forms two kinds of crystalline lattices, depending on the 3HV content. The 3HB-rich and 3HV-rich P(3HB-*co*-3HV)s were reported to form P(3HB) and P(3HV) homopolymer type crystalline lattice, respectively.[6−16] The studies on crystallization of P(3HB-*co*-3HV) showed the coexistence of both the 3HB and 3HV units in the P(3HB) and P(3HV) crystalline lattices.[6,16−20] It has been reported that the crystalline structural changes from one of the two isodimorphic crystals to another one for P(3HB-*co*-3HV) occurred in a rather broad range of 36−56 mol % 3HV.[13] The reason of this phenomenon had not been determined until recently. It has been recently found that the crystalline structural change occurs in a very narrow range of 3HV content between 47 and 52 mol % 3HV,[15] which confirmed that the coexistence of two crystalline lattices was caused by the incomplete fractionation of the copolymer samples.

Herein, continuing the preceding studies,[15] we investigate the thermal and crystalline structural characteristics of bacterial unfractionated and compositionally fractionated P(3HB-*co*-3HV) samples with high 3HV content.

Experimental Section

Materials. The biosyntheses of original unfractionated samples Ao, Bo, and Co were carried out by a two-stage fermentation of *R. eutropha* (ATCC17699, NCIB11599).[5,12] The first stage fermentation was performed in order to increase the bacterial cells in nutrient-rich medium containing 10 g/L of yeast extract, 10 g/L of polypeptone, 5 g/L of meat extract, and 5 g/L of $(NH_4)_2SO_4$. Then 15 g/L butyrate/valerate mixed carbon sources with a trace of nitrogen-free mineral components were used to biosynthesize P(3HB-*co*-3HV)s in the second stage.[5] The samples Do and Eo were biosynthesized from *n*-pentanol by mutant *Paracoccus denitrificans*.[21−23] The 3HV contents of the samples Ao, Bo, Co, Do, and Eo, determined by ^{1}H NMR spectra, were 45, 49, 70, 80, and 96 mol %, respectively. The crude samples were purified by reprecipitation with chloroform/methanol, and then chloroform/*n*-hexane solvent/nonsolvent systems, after being extracted from bacterial cells with hot chloroform using a Soxhlet apparatus.

The bacterial original P(3HB-*co*-3HV) samples were fractionated into fractions with different 3HV contents by fractional precipitation with chloroform/*n*-heptane. *n*-Heptane was carefully added into the copolyester/chloroform solution (starting polymer concentration 1 g/100 mL). Copolyester fractions were sampled by a constant ΔC of *n*-heptane in which ΔC means the incremental volumetric content of *n*-heptane in the mixed solvent between two continuous steps.[24]

P(3HB) was biosynthesized by *R. eutropha* from butyrate as a sole carbon source.[5] The two P(3HB-*co*-3HV) fractions with 14 and 52 mol % 3HV contents were obtained from the fractionation of an original copolymer with 3HV content of 47 mol %, which was also synthesized by *R. eutropha* from butyrate/valerate. The P(3HB-*co*-3HV) films cast from chloroform solution were melt at 195 °C and isothermally crystallized at 30 °C for at least 4 weeks before the measurements of DSC, WAXD and solid-state ^{13}C NMR.

Analytical Procedures. The ^{1}H NMR spectra were measured in $CDCl_3$ solution on a JEOL GSX-270 spectrometer at 270 MHz and 30 °C.[5] Tetramethylsilane was used as an internal chemical shift reference. The comonomer composition of the P(3HB-*co*-3HV) samples were determined by the ^{1}H NMR spectra from the relative peak intensities at about 0.9 and 1.3 ppm corresponded to the methyl group of 3HV and 3HB unit, respectively.

Weight-average molecular weight (M_w) and polydispersity (M_w/M_n) were characterized by a Tosoh HLC-8020 GPC system with a Tosoh SC-8010 controller, refractive detector, TSK GEL G20000Hxl, and GMMHxl columns. Polystyrene samples with narrow molecular-weight distribution were used as standards to calibrate the GPC curve.

DSC thermal analyses were performed on a Seiko DSC-220 assembled with a SSC-580 thermal controller. Isothermally crystallized polymer samples were pre-sealed in aluminum pans. DSC thermograms were recorded from −30 to +210 °C at heating rate of 10 °C/min (first heating scan). After rapidly quenching by liquid nitrogen, the samples were reheated from −100 to +195 °C at a heating rate of 20 °C/min (second heating scan). Melting point (T_m) was taken as the peak of endothermic curve recorded by the first heating scan, and the value of heat of fusion (ΔH) was calculated from the integral of the endothermic curve. Glass transition temperature (T_g) was estimated as the midpoint of heat capacity change in the thermal diagram measured by the second heating scan.

The wide-angle X-ray diffraction (WAXD) pattern was recorded in a θ range of 5−50° at a scanning speed of 1 °/min on a Rigaku RU-200 (50kV/180mA). The nickel-filtered Cu Kα X-ray radiation ($\lambda = 0.154\ 18$ nm) was used as the source. The degree of crystallinity was estimated according to the method developed by Vonk.[25]

The solid-state cross-polarization magic-angle spinning (CPMAS) ^{13}C NMR spectra were observed at 100 MHz using a Varian Unity-400 NMR spectrometer. The sample was inserted in a zirconia rotor and the spinning frequency was set at 4.0−6.0 kHz. All spectra were obtained with a contact time of 2.0 ms and a pulse delay of 10 s. The ^{13}C chemical shifts were referenced to the methyl resonance of hexamethylbenzene as the external standard (17.4 ppm from tetramethylsilane).

Table 1. Fractionation Results for P(3HB-*co*-3HV)

sample	solvent *n*-heptane, vol %	fw, %	3HV, mol %[a]	$M_w \times 10^5$ [b]	M_w/M_n[b]
Ao			45	5.17	2.66
A1	60	2.6	26	9.96	1.27
A2	62	25.8	26	6.56	1.38
A3	64	13.6	33	4.64	1.62
A4	66	15.4	47	11.2	2.04
A5	68	6.0	45	5.30	2.36
A6	70	18.2	56	5.26	2.40
A7	72	6.5	59	8.88	2.43
A8	74	5.4	60	2.02	1.62
A9	76	4.6	60	0.67	1.32
Bo			49	2.22	2.29
B1	62	5.2	27	3.15	1.86
B2	64	28.0	30	2.60	2.15
B3	66	16.9	32	2.61	2.17
B4	68	12.8	40	1.19	1.86
B5	70	9.5	48	1.89	2.00
B6	72	16.7	58	1.21	1.72
B7	74	8.4	68	1.35	2.27
Co			70	12.9	2.31
C1	68	6.4	30	15.5	1.76
C2	76	17.9	66	17.4	1.43
C3	78	29.7	68	20.0	1.76
C4	80	35.1	74	12.4	2.21
C5	82	21.4	74	14.2	1.90
Do			80	4.34	2.45
D1	66.7	3.8	93	3.99	2.21
D2	67.7	10.5	94	4.88	2.84
D3	70.0	35.8	94	4.30	2.75
D4	70.6	8.7	93	5.01	2.25
D5	71.4	4.1	89	5.46	2.02
D6	72.2	2.1	85	8.01	2.17
D7	73.0	1.8	81	5.67	2.87
D8	74.4	16.6	84	5.87	1.84
D9	75.0	3.7	80	6.66	1.68
D10	75.6	1.5	80	3.08	1.42
D11	76.2	4.2	80	1.34	1.68
D12	*c*	4.1	54	0.45	2.16
Eo			96	5.02	2.39
E1	67.7	22.4	98	4.15	2.67
E2	68.8	57.6	96	5.33	2.47
E3	70.0	2.9	97	5.63	3.08
E4	70.6	7.8	95	6.66	2.75
E5	71.4	1.4	91	7.07	1.78
E6	72.2	0.8	74	8.61	1.80
E7	73.0	3.2	75	9.58	1.67
E8	74.0	1.4	85	4.20	2.67

[a] Determined by ^{1}H NMR spectra. [b] Determined by GPC. [c] Collected by evaporating the solvent.

Results

Fractionation of P(3HB-*co*-3HV). Results of fractionation are tabulated in Table 1. The origial bacterial sample Ao with 45 mol % 3HV was fractionated into nine fractions when the concentration of *n*-heptane in the chloroform/*n*-heptane mixed solvent changed from 60 to 76 vol %. The 3HV content of the fractions increased from 26 to 60 mol % with the addition of *n*-heptane. Of the compositionally similar fractions (A1, A2 and A8, A9), the fractions with higher M_w (A1 and A8) were precipitated first.

In the case of the sample Bo, seven fractions were obtained when the concentration of *n*-heptane increased from 62 to 74 vol %. The 3HV contents of the fractions increased from the first fraction (27 mol %) to the last fraction (68 mol %). Although the M_w of the fractions decreased with the fraction number, they did not show continual change; thus, there is no explicit effect of molecular weight on the fractionation of the sample Bo.

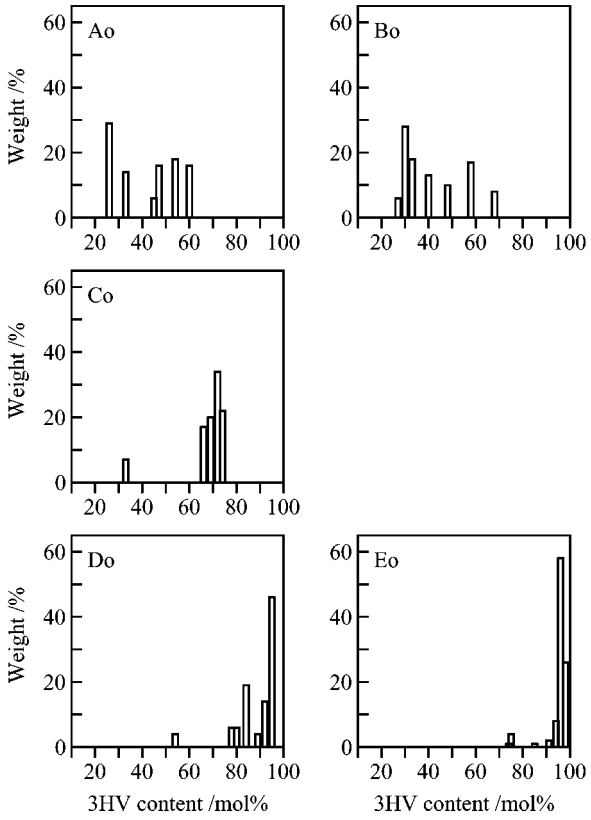

Figure 1. Fractionation results of P(3HB-*co*-3HV) with 3HV content of 45 (Ao), 49 (Bo), 70 (Co), 80 (Do), and 96 mol %(Eo).

The sample Co was fractionated into five fractions. The 3HV contents of C2 to C5 fractions were similar, ranged from 66 to 74 mol %, while the 3HV content of the first fraction C1 was the lowest (30 mol %). The M_w of these fractions were similar.

When the sample Do with 80 mol % 3HV was fractionated, the feature of fractionation behavior was quite different from those of other samples with lower 3HV content. Increasing the concentration of *n*-heptane, the 3HV content of the precipitated fractions decreased. This result is contrary to those of the samples Ao, Bo, and Co. The M_w of the last three fractions decreased with the fraction number, indicating some effect of molecular weight on the fractionation results.

The fractionation result of the sample Eo showed the same tendency as that of the sample Do. The 3HV content decreased from 98 mol % of the E1 fraction to 74 mol % of the E6 fraction with the addition of *n*-heptane, while the 3HV content of the last two fractions increased. From fractions E1 to E7, the M_w increased a little, while that of the last fraction, E8, decreased.

From Table 1, it was concluded that the effect of M_w on the fractionation is not large. Figure 1 shows the fractionation results of the five bacterial original samples. The samples Ao, Bo, Do, and Eo were fractionated into several fractions with different 3HV content, while the fractionation of the

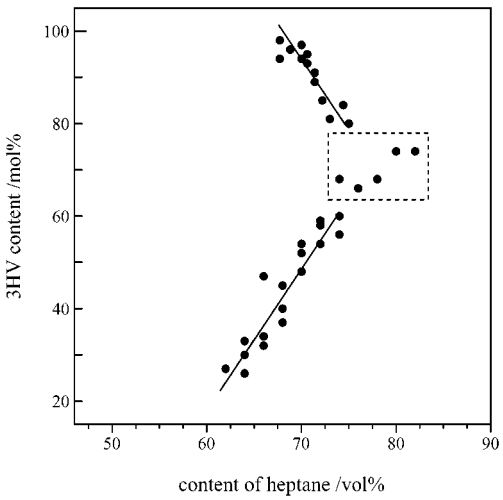

Figure 2. Plots of 3HV content vs *n*-heptane concentration of fractionated P(3HB-*co*-3HV) samples obtained by chloroform/*n*-heptane fractionation.

sample Co was not so completely. Although the samples Do and Eo were produced by biosynthesis from a sole carbon source, they also have broad CCD, which might be caused by the different pathways for the biosynthesis of the 3HB and 3HV units in PHA from *n*-pentanol.[22]

Figure 2 shows the plots of 3HV mol % vs *n*-heptane concentration from fractionation results. It is clear that the fractionation tendencies of P(3HB-*co*-3HV)s with 3HV content lower than 60 mol % and higher than 80 mol % are out of the ordinary. For samples with low 3HV content, addition of the *n*-heptane led to the earlier precipitation of P(3HB-*co*-3HV) with lower 3HV content. This result is the same as previously reported for bacterial P(3HB-*co*-3HV)s with low 3HV content.[8] For the samples with high 3HV content, addition of the *n*-heptane led to the precipitation from copolyester fraction with high 3HV content. This is just contrary to that with low 3HV content. These results indicated that, when the 3HV content of the original copolymer is between 60 and 80 mol %, it is difficult to fractionate the copolymers on the basis of the difference in comonomer composition by using chloroform/*n*-heptane solvent system.

Thermal Properties of Original and Fractionated Bacterial P(3HB-*co*-3HV)s. DSC thermal diagrams of the isothermally crystallized samples are shown in Figure 3. The first curve of each graph corresponds to the unfractionated original and the others to the fractionated samples. Comparing the curves of the fractions obtained from the samples Ao, Bo, Do, and Eo, it can be observed that the melting points (T_m) shift from high to low temperature with the fraction number except that the T_m values of the last or several last fractions increase a little, which may be caused by the remains of the preceding fractions. By varying the heating rate, it was evident that the two-peak melting behavior observed for several fractionated samples was due

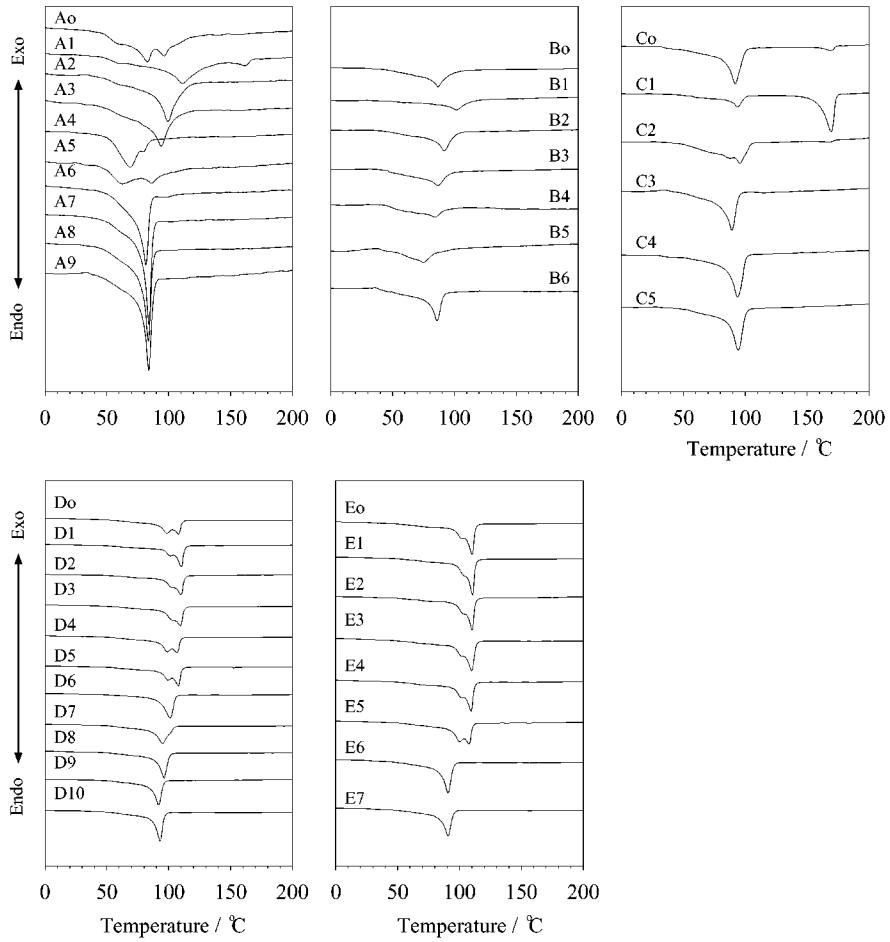

Figure 3. DSC melting curves for the isothermally crystallized original and fractionated samples recorded during the first heating scan.

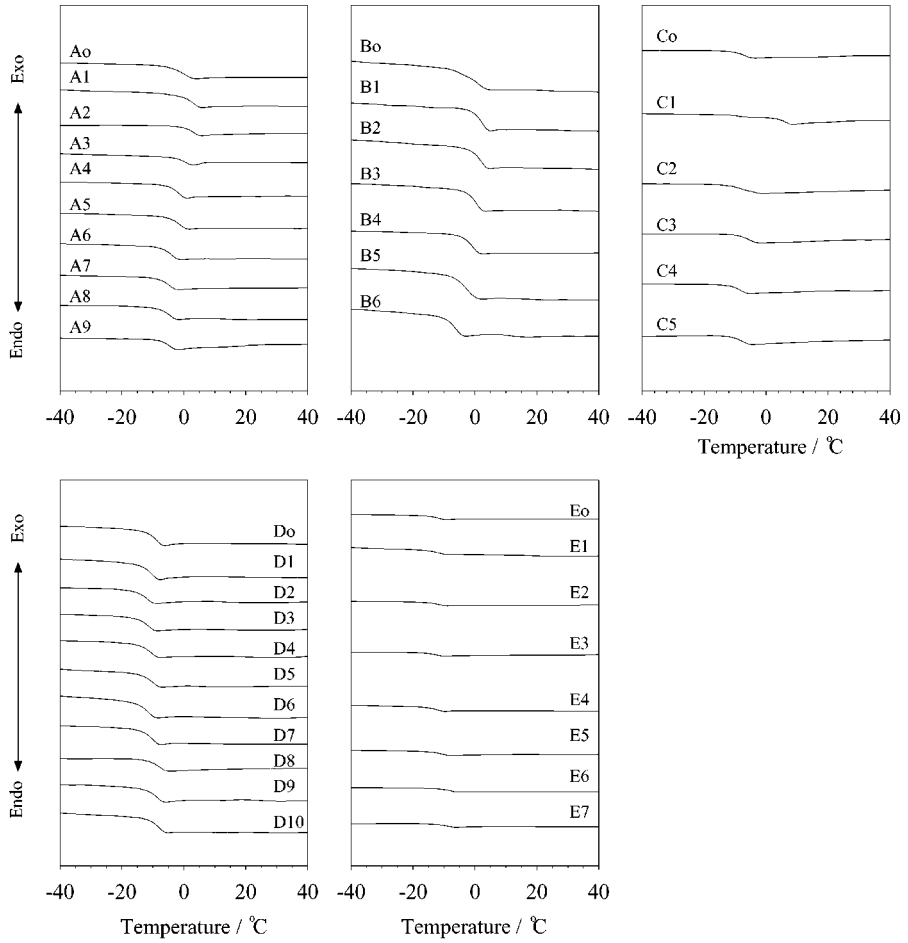

Figure 4. DSC curves for the original and fractionated samples recorded during the second heating scan.

to the recrystallization during DSC heating process.[8] Otherwise, the 3HV content-dependence of the melting points of the fractions obtained from the sample Co shows a zigzag tendency.

To clarify the behaviors of glass transition, the second heating scans of the original and fractionated samples were measured, and the results were shown in Figure 4. The T_g values of the fractions obtained from the samples Ao, Bo, and Co decreased with the fraction number, while those from the samples Do and Eo increased. On the other hand, for the original samples broader temperature ranges of the glass transition than those for the fractionated samples were observed.

To clarify the relationship between the 3HV content of P(3HB-*co*-3HV)s and their thermal properties, the plots of T_m, ΔH, and T_g against 3HV content of P(3HB-*co*-3HV)s are shown in Figure 5. The plots of T_m and ΔH show a ravine at the 3HV content between 40 and 50 mol %, which was considered to be the intermediate point of critical 3HV content range for crystalline structural change between the P(3HB) and the P(3HV) homopolymer-type crystalline lattice.[7,11,12] The first heating scan curves of some first fractions of the samples Ao and Co have two well-separated melting peaks, which may be caused by the coexistence of two main copolymer fractions with much different 3HV content copolymer. Of all the original and fractionated samples, the T_g value decreases with increasing of the 3HV content, indicating that the segmental mobility of copolymer chain in the amorphous phase is related to the comonomer compositions.

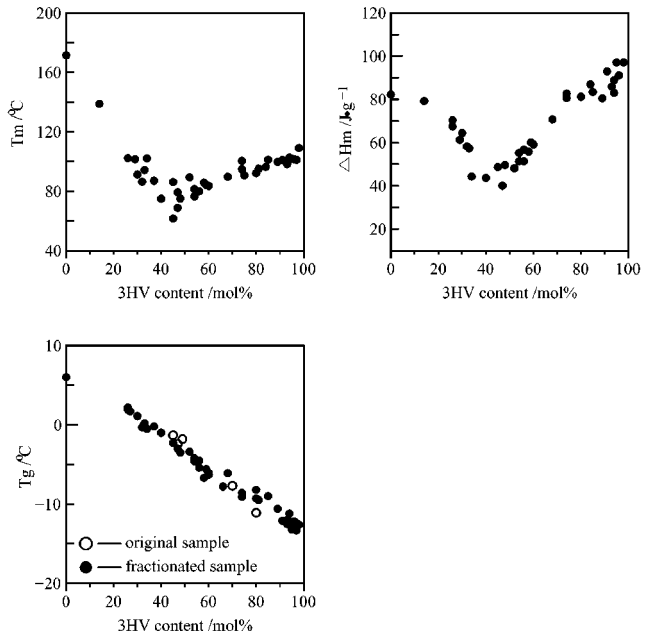

Figure 5. Plots of T_m, ΔH, and T_g vs 3HV content of original and fractionated P(3HB-co-3HV)s.

Crystalline Structures of Original and Fractionated P(3HB-*co*-3HV)s. Figure 6 shows the WAXD patterns of seven well-fractionated P(3HB-*co*-3HV) samples with 14−

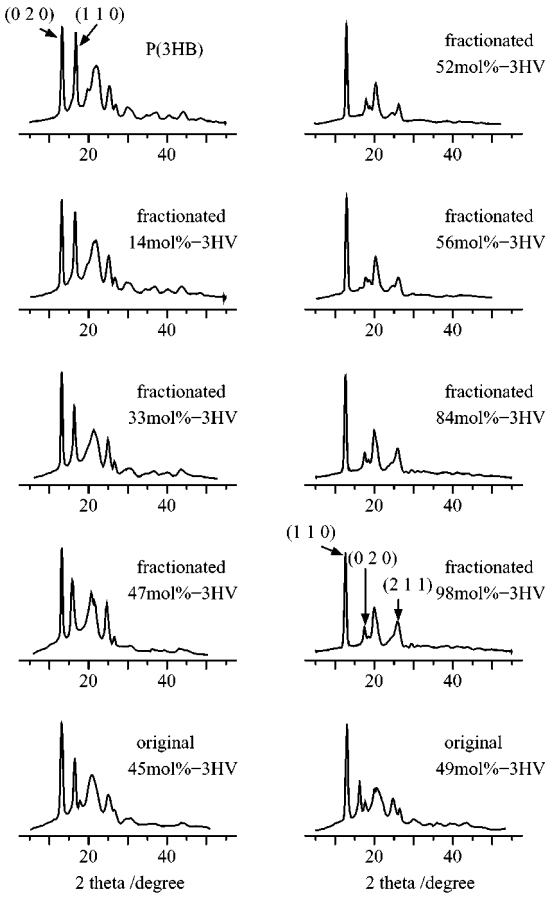

Figure 6. Wide-angle X-ray diffraction patterns for compositionally fractionated P(3HB-*co*-3HV) samples as well as P(3HB) and original unfractionated P(3HB-*co*-3HV) samples.

98 mol % 3HV content, P(3HB), and two original unfractionated samples with 45 and 49 mol % 3HV content. The peak at $2\theta = 17°$ corresponds to the (1 1 0) diffraction of the P(3HB) homopolymer-type lattice and that at $2\theta = 18°$ corresponds to the (0 2 0) of P(3HV)'s.[11−13,15,26−28] The fractionated samples with 3HV content of 0 [P(3HB)], 14, 33, and 47 mol %, i.e., lower than 47 mol %, form only the P(3HB)-type crystalline structure. As the 3HV content of the fractionated P(3HB-*co*-3HV) is higher than 52 mol % (52, 56, 84, and 98 mol %), only the P(3HV)-type crystalline structure is observed. However, in the WAXD patterns of original samples with 45 and 49 mol % 3HV content, both the P(3HB) and the P(3HV) type lattices are observed. It is clarified that the coexistence of both crystalline lattices found for the original samples is mainly due to the coexistence of copolymers with different comonomer composition.

The degrees of crystallinity of fractionated P(3HB-*co*-3HV)s with distinct composition were calculated from the WAXD patterns and plotted in Figure 7. The minimum value was observed in the comonomer composition range of 40−50 mol % 3HV. The value of 3HV content found for well-fractionated P(3HB-*co*-3HV) sample which shows the minimum crystallinity is clearly larger than that (30−40 mol % 3HV) reported in the previous paper.[13]

The lattice parameters *a*, *b*, and *c* of the P(3HB)- and P(3HV)-type crystalline lattices were calculated and plotted against the 3HV content in Figure 8. The values of these parameters were similar to those reported in the previous

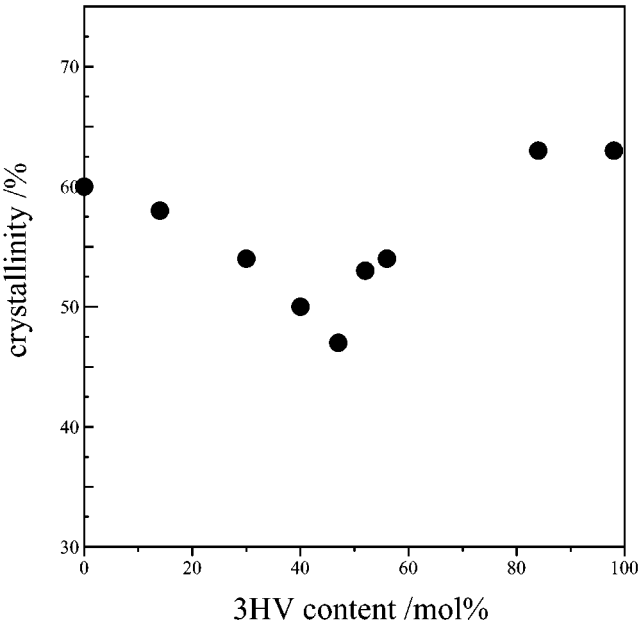

Figure 7. Degrees of crystallinity obtained from WAXD patterns of P(3HB) and fractionated P(3HB-*co*-3HV) samples plotted against 3HV content.

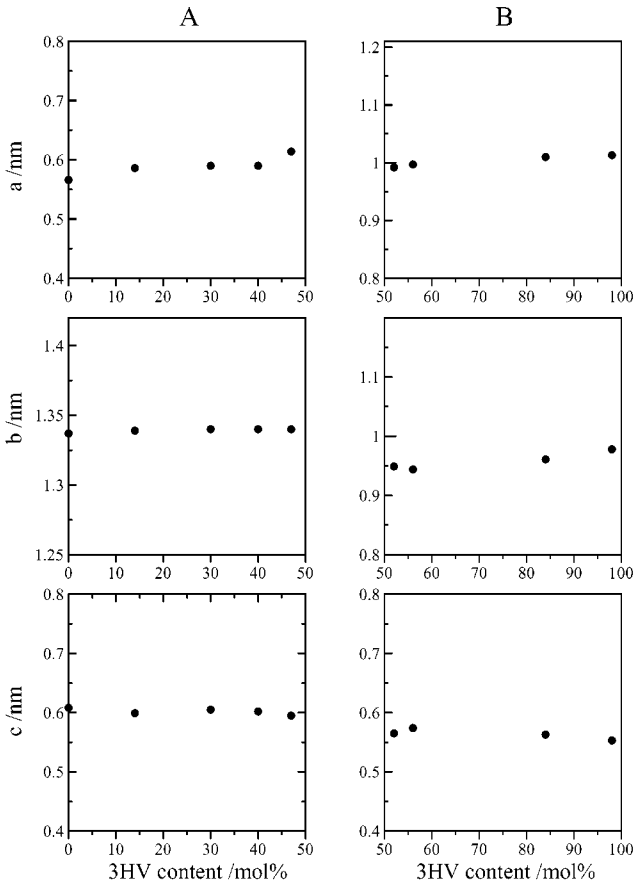

Figure 8. Unit cell parameters *a*, *b*, and *c* of the fractionated P(3HB-*co*-3HV) samples: (A) P(3HB)-type crystalline lattices; (B) P(3HV)-type crystalline lattices.

papers.[7,28] In the P(3HB)-type crystal phase, as shown in Figure 8A, with increasing the 3HV unit, the value of *a* increased a little, indicating that the 3HV unit cocrystallized into the P(3HB) crystalline lattice and loosened the lattice. However, those of *b* and *c* almost did not change. In the

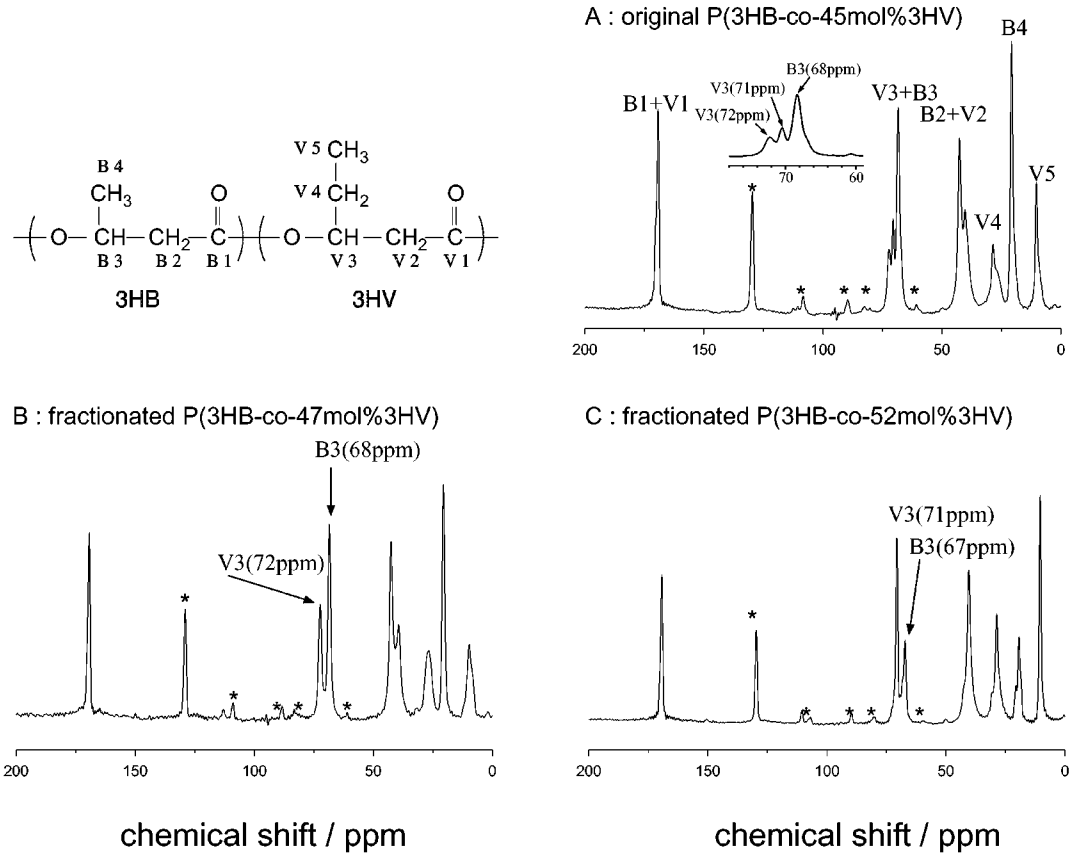

Figure 9. Solid-state CPMAS ^{13}C NMR spectra for original and fractionated P(3HB-*co*-3HV) samples with 3HV content near 50 mol %.

P(3HV)-type crystalline lattice shown in Figure 8B, the values of *a* and *b* increased a little and those of *c* were almost changeless with increasing the 3HV content, indicating the cocrystallization of 3HB unit in the P(3HV)-type crystalline lattice. With increasing 3HV unit content, the P(3HV)-type crystalline lattice becomes more compact.

The solid-state CPMAS ^{13}C NMR spectra of original P(3HB-*co*-45 mol %3HV) and fractionated copolymers with 47 and 52 mol % 3HV content are shown in Figure 9. At the temperature higher than T_g, the CP enhances more effectively the ^{13}C NMR signals arisen from the crystalline phase of P(3HB-*co*-3HV)s than those from the amorphous phase.[6] So, the signals appeared in the spectra of Figure 9 are considered to be mainly those from the crystalline phase. According to the assignments reported in the previous paper,[6] the signals at 72, 71, 68, and 67 ppm correspond to the methine carbon resonances of the 3HV unit in the P(3HB)-type lattice, the 3HV unit in the P(3HV)-type lattice, the 3HB unit in the P(3HB)-type lattice and the 3HB unit in the P(3HV)-type lattice, respectively. In the spectrum of fractionated P(3HB-*co*-47 mol %3HV) sample, only the resonances of the 3HB and 3HV methine carbons included in the P(3HB)-type crystalline lattice is observed. Thus, the ^{13}C NMR spectrum clearly indicates that P(3HB-*co*-47 mol %3HV) forms the P(3HB)-type crystal composed of not only the 3HB unit but also the 3HV unit. Otherwise, the ^{13}C NMR spectrum clearly indicates that fractionated P(3HB-*co*-52 mol %3HV) copolymer forms only the P(3HV)-type crystalline lattice including the 3HB unit as well as the 3HV unit, although the difference of 3HV content between P(3HB-*co*-47 mol %3HV) and P(3HB-*co*-52 mol %3HV) is only 5 mol %. While in the spectrum of the original unfractionated P(3HB-*co*-45 mol %3HV) copolymer, the methine resonances arisen from both the P(3HB)- and the P(3HV)-type crystalline lattice can be explicitly observed. The results of WAXD analysis and those of CPMAS ^{13}C NMR analysis are consistent with each other, and both of the results prove that the crystalline structural transition of bacterial P(3HB-*co*-3HV) samples occurred at a distinct change of comonomer composition between 47 and 52 mol % 3HV.

Discussion

Since Kamiya et al.[5] have indicated the complex comonomer compositions of the bacterially synthesized P(3HB-*co*-3HV)s by statistical analysis of sequence structures, comonomer compositional fractionations of bacterial P(3HB-*co*-3HV),[7,8] P(3HB-*co*-3HP),[24] and P(3HB-*co*-4HB)[29] have been investigated by using solvent/nonsolvent mixtures. The compositional fractionation of P(3HB-*co*-3HP) has been found to proceed mainly by difference in 3HP content. When P(3HB-*co*-3HP) of any 3HP content was fractionated with chloroform/*n*-heptane mixed solvent system, the 3HP content of the fractions decreased with the increasing of *n*-heptane concentration.[24,30,31]

Although no explicit relationship has been found between the concentration of acetone and the comonomer composition of P(3HB-*co*-3HV) fractions obtained by fractionation with acetone/water mixed solvent system, addition of water leads to the decreasing of 3HV content of the precipitated

fractions.[7,13] When the bacterial P(3HB-*co*-3HV)s were fractionated with chloroform/*n*-heptane mixed solvent system, the 3HV content of the precipitated fractions increased with the addition of *n*-heptane.[8] Up to now, the 3HV content of original unfractionated P(3HB-*co*-3HV)s, the comonomer compositional distributions of which have been investigated by fractionation with acetone/water and chloroform/*n*-heptane solvent/nonsolvent systems, were limited to less than 65[7,13] and 25 mol %,[8,20] respectively.

In the present study, we investigated the fractionation of P(3HB-*co*-3HV)s with 45, 49, 80, and 96 mol % 3HV content by chloroform/*n*-heptane mixed solvent system. The tendencies of the fractional precipitation of the P(3HB-*co*-3HV)s with 3HV content lower than 60 mol % and those with 3HV higher than 80 mol % were found to be contrary. Considering the polarity of the repeating unit of polymer chain and solvent system, the P(3HB-*co*-3HV) fractions gradually precipitated in the order of increasing 3HV content can be explained. Because the side chain of the 3HV unit is the ethyl group instead of the methyl group of the 3HB unit, the polarity of the P(3HB-*co*-3HV) chain depends on the comonomer composition.

The difference of crystallizability of P(3HB-*co*-3HV)s may also affect the precipitation. It has been reported that the 3HV content dependence of the spherulite growth rates of P(3HB-*co*-3HV)s shows behavior similar to that of the melting temperature.[8,32] It is inferable from Figure 5 that the spherulite growth rates of P(3HB-*co*-3HV)s also have a ravine at the 3HV content between 40 and 50 mol %. For P(3HB-*co*-3HV)s with low 3HV content (0−50 mol %) both of the polarity and the crystallizability decrease in paralled with increasing the 3HV content without contradictory. On the contrary, for P(3HB-*co*-3HV)s with 3HV content higher than 50 mol %, the effects of the polarity and the crystallizability on the precipitation conflict with each other. Namely, the polarity decreases but the crystallizability increases with increasing the 3HV content. It can be assessed that for 50−60 mol % 3HV samples, the effect of polarity takes precedence, while for the high 3HV samples(higher than 80 mol %), that of crystallizability takes. For the P(3HB-*co*-3HV) samples with 60−80 mol % 3HV, both the effects offset each other. Thus, the fractionation of P(3HB-*co*-3HV)s occurres as reported.

As mentioned in the Introduction, the 3HB-rich and 3HV-rich P(3HB-*co*-3HV)s form P(3HB)- and P(3HV)-type crystlline lattices, respectively. In the P(3HB-*co*-3HV)s with 3HV content near 50 mol % the two crystalline lattice types were coexistence. The well-fractionated samples with 3HV content near 50 mol % were obtained in the present study. Not only the WAXD pattern but also the solid-state CPMAS ^{13}C NMR spectra proved that the crystalline structural change occurs between 47 and 52 mol % 3HV content, which is much narrower than that found in the previous report.[13] This finding indicated that the coexistence of two types of crystalline lattices is caused by the broad comonomer compositional distribution.

Although it is difficult to analyze quantitatively the 3HV mol % content in the P(3HB)- or P(3HV)-type crystalline regions from the CPMAS ^{13}C NMR spectra shown in Figure 9, the methine carbon resonances clearly indicated that the 3HV and the 3HB units cocrystallized into the P(3HB)- and P(3HV)-type crystalline lattice, respectively. It has been well-known that the spatial symmetry of PHA crystals belongs to the $P2_12_12_1$ space group.[19] Because the 3HV unit has one more carbon atom in its side chain than the 3HB unit, the cocrystallization of the 3HV unit into the P(3HB)-type crystalline lattice will expand and loosen the lattice. Thus, the increase of the value of cell parameter *a* with the increase of the 3HV content ranging from 0 to 50 mol % can be easily explained. The analyses on lattice parameters from WAXD also drew the conclusion that increasing the 3HB content did not significantly influence the P(3HV) lattice, as reported.[19,33]

Conclusions

A series of microbial P(3HB-*co*-3HV) copolymers with relatively higher 3HV content were compositionaly fractionated by fractional precipitation methods using a mixed solvent of chloroform/*n*-heptane. The solvent composition dependence of the fractionation behavior of P(3HB-*co*-3HV)s with low 3HV content and that of ones with high 3HV content were found to be opposite. The *n*-heptane-induced fractional precipitation of the original P(3HB-*co*-3HV) samples with low 3HV content commenced from the fraction with low 3HV content, while that of original P(3HB-*co*-3HV) samples with high 3HV content commenced from the fraction with high 3HV content. Thus, not only the polarity but also the crystallizability would influence the fractionation of the copolymer. All bacterial P(3HB-*co*-3HV) samples investigated here were found to have broad comonomer compositional distribution. The minimum T_m and ΔH values were observed at 40−50 mol % 3HV content. For whole 3HV content range, the T_g value decreased with the increasing of 3HV content. The results of WAXD and CPMAS ^{13}C NMR analyses proved that the crystalline structural change occurrs in a very narrow range of 3HV content at 47−52 mol % 3HV. The cocrystallization occurred in both the P(3HB)- and P(3HV)-type crystalline lattices.

Acknowledgment. This research was partly supported by a Grant-in-Aid for Scientific Research on Priority Area, "Sustainalble Biodegradable Plastics", No. 11217204 (2000), from the Ministry of Education, Culture, Sports, Science, and Technology (Japan).

References and Notes

(1) Doi, Y.; Segawa, A.; Nakamura, S.; Kunioka, M. Production of biodegradable copolyesters by *Alcaligenes eutrophus*. In *Novel Biodegradable Microbial Polymers*; Dawes, E. A., Ed.; Kluwer Academic Publishers: Dordrecht, The Netherlands, 1990; pp 37−48.
(2) Braunegg, G.; Lefebvre, G.; Genser, K. F. *J. Biotechnol.* **1998**, *65*, 127−161.
(3) Yoshie, N.; Inoue, Y. *Int. J. Biol. Macromol.* **1999**, *25*, 193−200.
(4) Inoue, Y. *J. Mol. Struct.* **1998**, *441*, 119−127.
(5) Kamiya, N.; Yamamoto, Y.; Inoue, Y.; Chûjô, R.; Doi, Y. *Macromolecules* **1989**, *22*, 1676−1682.
(6) Kamiya, N.; Sakurai, M.; Inoue, Y.; Chûjô, R.; Doi, Y. *Macromolecules* **1991**, *24*, 2178−2182.
(7) Mitomo, H.; Morishita, N.; Doi, Y. *Macromolecules* **1993**, *26*, 5809−5811.
(8) Yoshie, N.; Menju, H.; Sato, H.; Inoue, Y. *Macromolecules* **1995**, *28*, 6516−6521.

(9) Fred, W.; Billmeyer, J. Fractionation of Polymers. In *Textbook of Polymer Science*; Wiley Int. Ed.; Interscience Publishers: John Wiley and Sons: New York and London, 1962; pp 47−51.
(10) Steinbüchel, A.; Debzi, E.; Marchessault, R. H.; Timm, A. *Appl. Microbiol. Biotechnol.* **1993**, *39*, 443−449.
(11) Bluhm, T. L.; Hamer, G. K.; Marchessault, R. H.; Fyfe, C. A.; Veregin, R. P. *Macromolecules* **1986**, *19*, 2871−2876.
(12) Kunioka, M.; Tamaki, A.; Doi, Y. *Macromolecules* **1989**, *22*, 694−697.
(13) Mitomo, H.; Morishita, N.; Doi, Y. *Polymer* **1995**, *36*, 2573−2578.
(14) Mitomo, H.; Takahashi, T.; Ito, H.; Saito, T. *Int. J. Biol. Macromol.* **1999**, *24*, 311−318.
(15) Yamada, S.; Wang, Y.; Asakawa, N.; Yoshie, N.; Inoue, Y. *Macromolecules* **2001**, *34*, 4659−4661.
(16) Kamiya, N.; Sakurai, M.; Inoue, Y.; Chûjô, R. *Macromolecules* **1991**, *24*, 3888−3892.
(17) Yoshie, N.; Sakurai, M.; Inoue, Y.; Chûjô, R. *Macromolecules* **1992**, *25*, 2046−2048.
(18) VanderHart, D. L.; Orts, W. J.; Marchessault, R. H. *Macromolecules* **1995**, *28*, 6394−6400.
(19) Barker, P. A.; Mason, F.; Barham, P. J. *J. Mater. Sci.* **1990**, *25*, 1952−1956.
(20) Saito, M.; Inoue, Y.; Yoshie, N. *Polymer* **2001**, *42*, 5573−5580.
(21) Yamane, T.; Chen, X. F.; Ueda, S. *FEMS Microbiol. Lett.* **1996**, *135*, 207−211.
(22) Yamane, T.; Chen, X. F.; Ueda, S. *Appl. Environ. Microbiol.* **1996**, *62*, 380−384.
(23) Maehara, A.; Ikai, K.; Ueda, S.; Yamane, T. *Biotechnol. Bioengin.* **1998**, *60*, 61−69.
(24) Cao, A.; Ichikawa, M.; Kasuya, K.; Yoshie, N.; Asakawa, N.; Inoue, Y.; Doi, Y. *Polym. J.* **1996**, *28*, 1096−1102.
(25) Vonk, C. G. *J. Appl. Crystallogr.* **1973**, *6*, 148−152.
(26) Yokouchi, M.; Chatani, Y.; Tadokoro, H.; Teranishi, K.; Tani, H. *Polymer* **1973**, *14*, 267−272.
(27) Yokouchi, M.; Chatani, Y.; Tadokoro, H.; Tani, H. *Polym. J.* **1974**, *6*, 248−255.
(28) Iwata, T.; Doi, Y. *Macromolecules* **2000**, *33*, 5559−5565.
(29) Mitomo, H.; Hsieh, W. C.; Nishiwaki, K.; Kasuya, K.; Doi, Y. *Polymer* **2001**, *42*, 3455−3461.
(30) Cao, A.; Kasuya, K.; Abe, H.; Doi, Y.; Inoue, Y. *Polymer* **1998**, *39*, 4801−4816.
(31) Wang, Y.; Ichikawa, M.; Cao, A.; Yoshie, N.; Inoue, Y. *Macromol. Chem. Phys.* **1999**, *200*, 1047−1053.
(32) Scandola, M.; Ceccorulli, G.; Pizzoli, M.; Gazzano, M. *Macromolecules* **1992**, *25*, 1405−1410.
(33) Barker, P. A.; Barham, P. J.; Martinez-Salazar, J. *Polymer* **1997**, *38*, 913−919.

BM010128O